

Theoretical Framework of Project

Baselines for Gauge-Simulation Workstream (Schwinger / lattice dynamics) and Open-Quantum-Systems Workstream (pNRQCD-inspired Lindblad)

Overview

Validation Baseline establishes two theoretical pillars:

1. **Classical lattice gauge benchmark (pure gauge U(1) in 1+1D / 2D Euclidean):**
A Monte Carlo simulation is validated against an *exact* area-law result for Wilson loops. This serves as a correctness check for lattice gauge methodology.
2. **Hamiltonian Schwinger model baseline (gauge fields eliminated):**
The “integrated” spin-chain Hamiltonian is derived by enforcing Gauss’s law and expressing the electric field entirely in terms of matter (fermion) charges. This produces long-range interactions and forms the starting point for ED/VQE and real-time dynamics.

In parallel, Validation Baseline sets up the **Open Quantum System (OQS)** description used in the Brambilla–Vairo program for quarkonium in a medium: a Lindblad equation describing **singlet–octet transitions** driven by chromo-electric dipole interactions.

1. Pure Gauge U(1) in 2D: Wilson Loops and the Exact Area Law

Lattice formulation

Consider a 2D Euclidean lattice with $U(1)$ link variables (parallel transporters)

$$U_\ell \equiv U_{x,\mu} = e^{i\theta_{x,\mu}}, \quad \theta_{x,\mu} \in (-\pi, \pi].$$

Under a local gauge transformation $g_x = e^{i\alpha_x}$, links transform as

$$U_{x,\mu} \rightarrow g_x U_{x,\mu} g_{x+\hat{\mu}}^{-1},$$

so the action must be built from **local gauge-invariant** combinations of links. The smallest such object is the plaquette variable

$$U_p \equiv U_{x,\mu} U_{x+\hat{\mu},\nu} U_{x+\hat{\nu},\mu}^{-1} U_{x,\nu}^{-1} = e^{i\theta_p},$$

where the plaquette angle is the oriented sum of link angles around plaquette p ,

$$\theta_p = \theta_{x,\mu} + \theta_{x+\hat{\mu},\nu} - \theta_{x+\hat{\nu},\mu} - \theta_{x,\nu}.$$

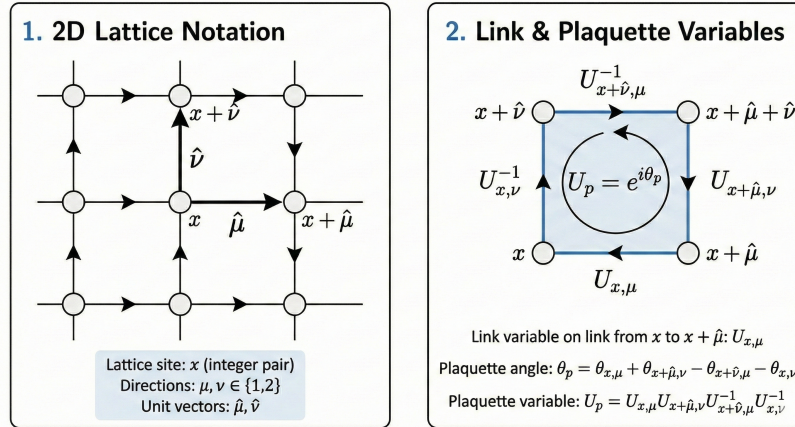
The standard Wilson choice for the lattice gauge action is proportional to the real part of U_p ,

$$\text{Re } U_p = \frac{1}{2} (U_p + U_p^*) = \cos \theta_p,$$

so the Wilson action is

$$S[U] = -\beta \sum_p \text{Re } U_p = -\beta \sum_p \cos(\theta_p).$$

(Equivalently one often writes $S'[U] = \beta \sum_p (1 - \cos \theta_p)$, which differs only by an additive constant. In the smooth-field limit $\theta_p \simeq a^2 F_{\mu\nu}$ and $1 - \cos \theta_p \simeq \theta_p^2/2$, reproducing $\int d^2x F_{\mu\nu}^2$ up to normalization.)



Wilson loop observable

For a closed loop C (e.g. a rectangle of size $R \times T$), the Wilson loop is the product of link variables along C ,

$$W(C) = \prod_{\ell \in C} U_\ell.$$

It is gauge invariant because the site phases cancel around a closed contour. For $U(1)$, $U_\ell = e^{i\theta_\ell}$ and the group is abelian, so

$$W(C) = \prod_{\ell \in C} e^{i\theta_\ell} = e^{i \sum_{\ell \in C} \theta_\ell},$$

with reversed orientations contributing $U_\ell^{-1} = e^{-i\theta_\ell}$. Its expectation value diagnoses confinement through an area law,

$$\langle W(R, T) \rangle \sim e^{-\sigma A}, \quad A = RT.$$

Exact result in 2D U(1)

In two-dimensional pure gauge $U(1)$, the Wilson loop depends only on the enclosed area (number of plaquettes) A . There are two complementary ways to see this.

(A) Geometric view: lattice Stokes' theorem + factorization Let Σ be a set of plaquettes filling the loop, $C = \partial\Sigma$. Because each interior link appears twice with opposite orientation, the product of plaquettes over Σ collapses to the boundary product:

$$\prod_{p \in \Sigma} U_p = \prod_{\ell \in \partial\Sigma} U_\ell = W(C).$$

In 2D pure gauge theory there are no propagating local degrees of freedom, and one can gauge-fix so that the remaining local variables are effectively the plaquette angles; the action is a sum of single-plaquette terms. For an observable that is a product of plaquettes in Σ , the expectation value factorizes:

$$\langle W(C) \rangle = \left\langle \prod_{p \in \Sigma} U_p \right\rangle = \prod_{p \in \Sigma} \langle U_p \rangle = \langle U_p \rangle^A.$$

The single-plaquette average is

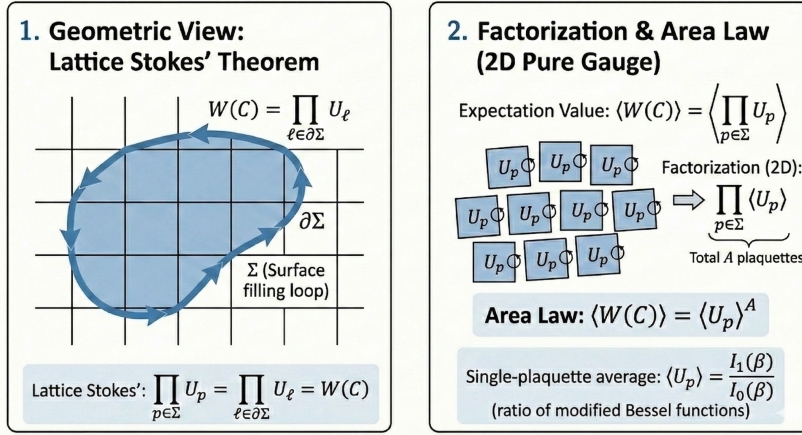
$$\langle U_p \rangle = \frac{\int_{-\pi}^{\pi} d\theta e^{\beta \cos \theta} e^{i\theta}}{\int_{-\pi}^{\pi} d\theta e^{\beta \cos \theta}} = \frac{I_1(\beta)}{I_0(\beta)},$$

using

$$I_n(\beta) = \frac{1}{2\pi} \int_{-\pi}^{\pi} d\theta e^{\beta \cos \theta} e^{in\theta}.$$

Hence

$$\langle W(A) \rangle = \left(\frac{I_1(\beta)}{I_0(\beta)} \right)^A.$$



(B) Character-expansion view: Fourier/Bessel expansion + link integrations Start from the partition function

$$Z = \int \prod_{\ell} \frac{d\theta_{\ell}}{2\pi} \prod_p e^{\beta \cos \theta_p}.$$

Use the $U(1)$ character (Fourier/Bessel) expansion on each plaquette:

$$e^{\beta \cos \theta_p} = \sum_{n_p \in \mathbb{Z}} I_{n_p}(\beta) e^{in_p \theta_p}.$$

Then

$$Z = \sum_{n_p} \left(\prod_p I_{n_p}(\beta) \right) \int \prod_{\ell} \frac{d\theta_{\ell}}{2\pi} \exp \left(i \sum_p n_p \theta_p \right).$$

Since θ_p is an oriented sum of link angles, one can write $\theta_p = \sum_{\ell} s_{p\ell} \theta_{\ell}$ with $s_{p\ell} \in \{0, \pm 1\}$, so

$$\sum_p n_p \theta_p = \sum_{\ell} \theta_{\ell} \left(\sum_p s_{p\ell} n_p \right).$$

Each link integral enforces a Kronecker delta constraint,

$$\int_{-\pi}^{\pi} \frac{d\theta_{\ell}}{2\pi} e^{im_{\ell} \theta_{\ell}} = \delta_{m_{\ell}, 0}, \quad m_{\ell} = \sum_p s_{p\ell} n_p,$$

so

$$Z = \sum_{n_p} \left(\prod_p I_{n_p}(\beta) \right) \prod_{\ell} \delta_{\sum_p s_{p\ell} n_p, 0}.$$

On a simply-connected lattice with trivial boundary sector, these constraints force $n_p = 0$ for all plaquettes, giving

$$Z = I_0(\beta)^{N_p},$$

where N_p is the total number of plaquettes.

For the Wilson loop,

$$\langle W(C) \rangle = \frac{1}{Z} \int \prod_{\ell} \frac{d\theta_{\ell}}{2\pi} \exp \left(i \sum_{\ell \in C} \theta_{\ell} \right) \prod_p e^{\beta \cos \theta_p}.$$

Introduce a link “current” $j_{\ell} \in \{0, \pm 1\}$ so that $W(C) = \exp(i \sum_{\ell} j_{\ell} \theta_{\ell})$. Repeating the same expansion and link integrations yields

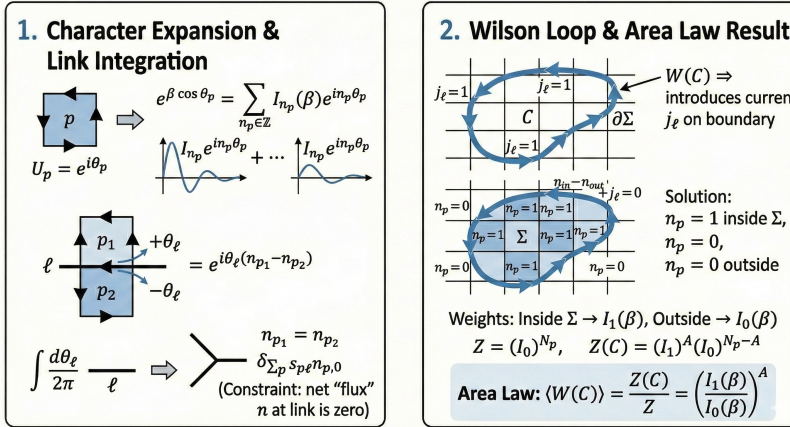
$$Z(C) \equiv \langle W(C) \rangle Z = \sum_{n_p} \left(\prod_p I_{n_p}(\beta) \right) \prod_{\ell} \delta_{\sum_p s_{p\ell} n_p + j_{\ell}, 0}.$$

In 2D, a solution of these constraints is $n_p = 1$ for p inside the loop ($p \in \Sigma$) and $n_p = 0$ outside, which implements that j is the boundary of Σ . This gives

$$Z(C) = I_1(\beta)^A \cdot I_0(\beta)^{N_p - A}.$$

Dividing by $Z = I_0(\beta)^{N_p}$,

$$\langle W(A) \rangle = \frac{Z(C)}{Z} = \left(\frac{I_1(\beta)}{I_0(\beta)} \right)^A.$$



Area law and string tension

Therefore,

$$-\ln \langle W(A) \rangle = A \ln \left(\frac{I_0(\beta)}{I_1(\beta)} \right) \equiv \sigma(\beta) \cdot A, \quad \sigma(\beta) = \ln \left(\frac{I_0(\beta)}{I_1(\beta)} \right).$$

Baseline: this exact area law provides a stringent unit test of the Monte Carlo update and Wilson-loop measurement pipeline.

2. The Schwinger Model on a Quantum Computer: Eliminating Gauge Redundancy

The central computational challenge of simulating a lattice gauge theory on a quantum computer is the size of the Hilbert space. A naive encoding of the (1+1) dimensional Schwinger model places one fermionic mode ψ_n on each of N lattice sites and one U(1) link variable $U_n = e^{i\theta_n}$ with conjugate electric field E_n on each of the $N-1$ links between them.

Each link lives in an infinite-dimensional rotor Hilbert space spanned by electric-field eigenstates $|E_n = \ell\rangle$ with $\ell \in \mathbb{Z}$, so a practical simulation must truncate the link Hilbert space to some finite dimension d per link, giving a total Hilbert space of dimension $2^N d^{N-1}$.

In one spatial dimension, however, a remarkable simplification is possible: the gauge field has no independent propagating degrees of freedom, and with open boundaries Gauss's law determines the electric field in terms of the matter content and boundary fluxes. This allows us to eliminate the gauge degrees of freedom entirely and reduce the problem to N qubits with Hilbert space dimension 2^N , avoiding link truncation altogether. This section carries out that elimination in detail, since the resulting integrated spin-chain Hamiltonian is the starting point for all subsequent variational and dynamical simulations.

Throughout this section we adopt the following index conventions: lattice sites are labelled $n = 0, 1, \dots, N-1$, and the link connecting site n to site $n+1$ carries the link variable U_n and electric field E_n , so links are labelled $n = 0, 1, \dots, N-2$. We additionally introduce boundary electric fields

$$E_{-1} \equiv E_L^{\text{bg}} \quad E_{N-1} \equiv E_R^{\text{bg}},$$

representing the flux entering the chain from the left and the flux exiting the chain to the right. Fixing E_L^{bg} and E_R^{bg} specifies a superselection sector corresponding to a choice of external static charges at the boundaries.

2.1 The lattice Hamiltonian

The Kogut–Susskind Hamiltonian for the Schwinger model with staggered fermions has three terms

$$H = H_{\text{hop}} + H_m + H_E.$$

The gauge-covariant hopping couples nearest-neighbour sites through the link

$$H_{\text{hop}} = -w \sum_{n=0}^{N-2} (\psi_n^\dagger U_n \psi_{n+1} + \text{h.c.}),$$

the staggered mass term assigns alternating energies to occupied sites

$$H_m = m \sum_{n=0}^{N-1} (-1)^n \psi_n^\dagger \psi_n,$$

and the electric energy penalises nonzero flux on each link

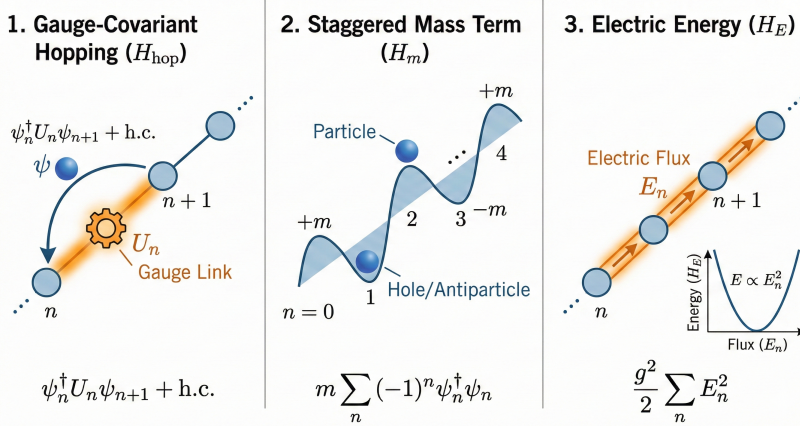
$$H_E = \frac{g^2}{2} \sum_{n=0}^{N-2} E_n^2.$$

There is no magnetic plaquette term because a single spatial dimension admits no closed loops of links. In one dimension the gauge field therefore has no independent propagating degrees of freedom: the absence of plaquettes means there is no magnetic dynamics, and Gauss's law fixes the remaining electric field given the matter configuration and boundary fluxes.

The link variable U_n enters the hopping to ensure local gauge invariance. Under a site-dependent $U(1)$ transformation $\psi_n \rightarrow e^{i\alpha_n} \psi_n$, the bilinear $\psi_n^\dagger \psi_{n+1}$ picks up a phase $e^{-i(\alpha_n - \alpha_{n+1})}$. The link transforms as $U_n \rightarrow e^{i(\alpha_n - \alpha_{n+1})} U_n$, so the combination $\psi_n^\dagger U_n \psi_{n+1}$ is invariant

$$\psi_n^\dagger U_n \psi_{n+1} \rightarrow \psi_n^\dagger e^{-i\alpha_n} e^{i(\alpha_n - \alpha_{n+1})} U_n e^{i\alpha_{n+1}} \psi_{n+1} = \psi_n^\dagger U_n \psi_{n+1}.$$

This is the minimal nearest-neighbour coupling compatible with the local symmetry.



2.2 Gauss's law and the elimination of gauge fields

Local gauge invariance implies a constraint on every physical state. On the lattice, the generator of gauge transformations at site n is the Gauss operator

$$G_n = E_n - E_{n-1} - \rho_n,$$

and physical states satisfy $G_n |\text{phys}\rangle = 0$, equivalently

$$E_n - E_{n-1} = \rho_n \quad n = 0, 1, \dots, N-1,$$

with the boundary conventions $E_{-1} = E_L^{\text{bg}}$ and $E_{N-1} = E_R^{\text{bg}}$.

The charge density ρ_n is defined with a staggered background subtraction

$$\rho_n = n_n - \frac{1 - (-1)^n}{2},$$

where $n_n = \psi_n^\dagger \psi_n$ is the occupation number. Since $\frac{1}{2}[1 - (-1)^n]$ equals 0 on even sites and 1 on odd sites, this gives

$$\rho_n = \begin{cases} n_n & n \text{ even,} \\ n_n - 1 & n \text{ odd.} \end{cases}$$

The motivation for this subtraction is that it makes the staggered vacuum locally neutral, $\rho_n = 0$ site by site, which avoids an extensive electric-field energy in the reference sector.

Because Gauss's law is a recursion relation $E_n = E_{n-1} + \rho_n$, iterating from the left boundary determines the electric field on every physical link in terms of the matter content

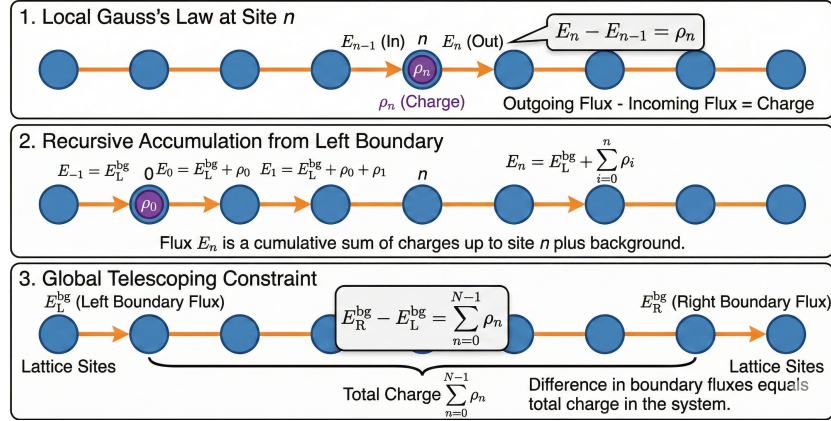
$$E_n = E_L^{\text{bg}} + \sum_{i=0}^n \rho_i \quad n = 0, 1, \dots, N-2.$$

Imposing Gauss's law at the final site $n = N-1$ yields the global telescoping constraint

$$E_R^{\text{bg}} - E_L^{\text{bg}} = \sum_{n=0}^{N-1} \rho_n,$$

which ties the difference of boundary fluxes to the total charge of the dynamical matter fields. This relation makes precise in what sense the boundary data label superselection sectors: changing E_L^{bg} and E_R^{bg} corresponds to changing the net external charge configuration at the boundaries.

Flux Recursion as a “Running Sum” along the Chain



With E_n fully determined on the links, we substitute back into the electric energy

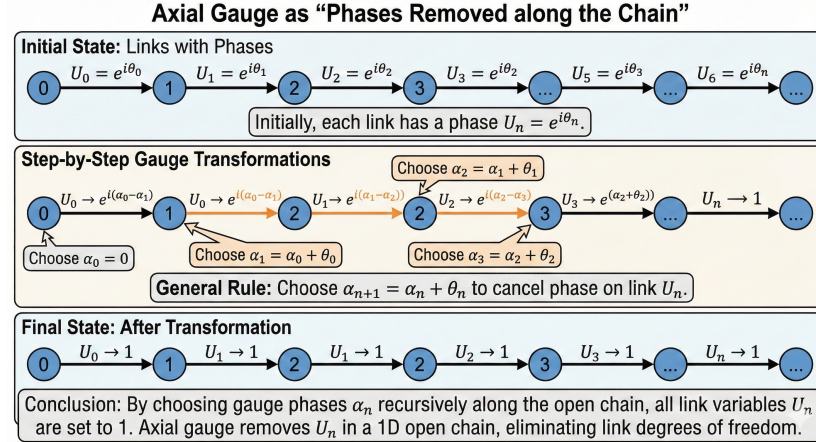
$$H_E = \frac{g^2}{2} \sum_{n=0}^{N-2} \left(E_L^{\text{bg}} + \sum_{i=0}^n \rho_i \right)^2.$$

Expanding the square,

$$\left(E_L^{\text{bg}} + \sum_{i=0}^n \rho_i \right)^2 = (E_L^{\text{bg}})^2 + 2E_L^{\text{bg}} \sum_{i=0}^n \rho_i + \sum_{i=0}^n \sum_{j=0}^n \rho_i \rho_j,$$

reveals that the electric energy becomes a long-range density-density interaction: every pair of charges ρ_i and ρ_j is coupled through the outermost sum over links n . This long-range character is the price of elimination: removing gauge degrees of freedom transfers the gauge-mediated interaction onto the matter sector as a nonlocal coupling.

Simultaneously, we use the gauge freedom to set $U_n = 1$ on every link by working in axial gauge. With open boundaries this is always possible by choosing gauge phases recursively so that $\alpha_{n+1} = \alpha_n + \theta_n$. With periodic boundaries a global Wilson loop $\prod_n U_n$ survives and cannot be gauged away, so we work exclusively with open boundaries. With all link variables removed and E_n expressed through the matter fields, the Hamiltonian acts on a purely fermionic Hilbert space of dimension 2^N .



2.3 Jordan–Wigner mapping to a spin chain

To map the fermionic Hilbert space onto qubits, we apply the Jordan–Wigner transformation. In the computational basis where $|0\rangle$ is empty and $|1\rangle$ is occupied, the Pauli Z operator acts as $Z_n|0\rangle = +|0\rangle$ and $Z_n|1\rangle = -|1\rangle$, so the number operator is

$$n_n = \frac{1 - Z_n}{2}.$$

The charge density then takes the compact form

$$\rho_n \equiv n_n - \frac{1 - (-1)^n}{2} = \frac{1 - Z_n}{2} - \frac{1 - (-1)^n}{2} = \frac{(-1)^n - Z_n}{2}.$$

For the hopping term, we use the Jordan–Wigner map for sites ordered left to right

$$\psi_n = \left(\prod_{k=0}^{n-1} Z_k \right) \sigma_n^- \quad \psi_n^\dagger = \left(\prod_{k=0}^{n-1} Z_k \right) \sigma_n^+,$$

where σ_n^\pm act only on site n . For nearest neighbours the Jordan–Wigner strings cancel, so the Hermitian hopping becomes the local flip–flop operator

$$\psi_n^\dagger \psi_{n+1} + \psi_{n+1}^\dagger \psi_n \longleftrightarrow \sigma_n^+ \sigma_{n+1}^- + \sigma_n^- \sigma_{n+1}^+.$$

Using $\sigma^\pm = \frac{X \pm iY}{2}$, this can be rewritten as the standard XY coupling

$$\sigma_n^+ \sigma_{n+1}^- + \sigma_n^- \sigma_{n+1}^+ = \frac{1}{2}(X_n X_{n+1} + Y_n Y_{n+1}).$$

Therefore

$$\psi_n^\dagger \psi_{n+1} + \text{h.c.} \longleftrightarrow \frac{1}{2}(X_n X_{n+1} + Y_n Y_{n+1}).$$

This mapping is especially transparent in the two-qubit basis on sites $(n, n+1)$,

$$|00\rangle, |01\rangle, |10\rangle, |11\rangle,$$

where $|0\rangle$ denotes empty and $|1\rangle$ denotes occupied. Writing $\sigma^+ = |1\rangle\langle 0|$ and $\sigma^- = |0\rangle\langle 1|$, the flip–flop operator

$$F \equiv \sigma_n^+ \sigma_{n+1}^- + \sigma_n^- \sigma_{n+1}^+$$

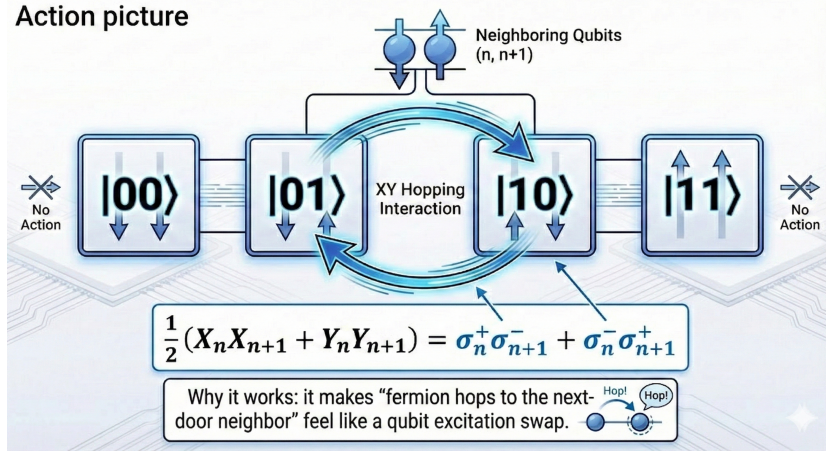
acts as

$$F|01\rangle = |10\rangle \quad F|10\rangle = |01\rangle \quad F|00\rangle = 0 \quad F|11\rangle = 0,$$

so it swaps the single-excitation states $|01\rangle$ and $|10\rangle$ while leaving $|00\rangle$ and $|11\rangle$ unchanged. Equivalently,

$$\frac{1}{2}(X_n X_{n+1} + Y_n Y_{n+1})|01\rangle = |10\rangle \quad \frac{1}{2}(X_n X_{n+1} + Y_n Y_{n+1})|10\rangle = |01\rangle,$$

with the operator annihilating $|00\rangle$ and $|11\rangle$. This makes the physical meaning of the fermion hopping term immediate: it moves a single occupation between neighbouring sites.



The **mass term** is diagonal

$$H_m = m \sum_{n=0}^{N-1} (-1)^n \frac{1 - Z_n}{2},$$

which acts as a staggered longitudinal field up to an additive constant.

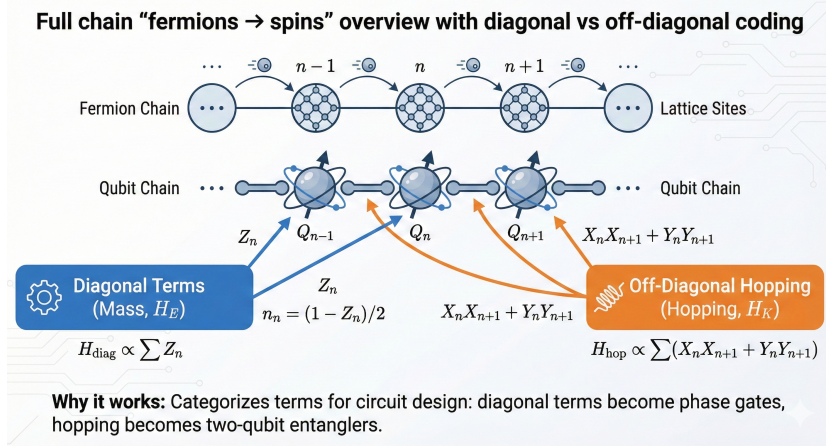
The **electric term** is also diagonal in the Z basis but nonlocal, since each term involves a cumulative sum

$$H_E = \frac{g^2}{2} \sum_{n=0}^{N-2} \left(E_L^{\text{bg}} + \sum_{i=0}^n \frac{(-1)^i - Z_i}{2} \right)^2.$$

Collecting these three pieces, the final spin-chain Hamiltonian is

$$H = -\frac{w}{2} \sum_{n=0}^{N-2} (X_n X_{n+1} + Y_n Y_{n+1}) + m \sum_{n=0}^{N-1} (-1)^n \frac{1 - Z_n}{2} + \frac{g^2}{2} \sum_{n=0}^{N-2} \left(E_L^{\text{bg}} + \sum_{i=0}^n \frac{(-1)^i - Z_i}{2} \right)^2$$

which acts on N qubits with Gauss’s law satisfied by construction.



Local gauge redundancy has been eliminated. The remaining continuous symmetry is global charge conservation, meaning that the dynamics cannot change the net U(1) charge carried by the dynamical matter fields. The conserved total charge is

$$Q = \sum_{n=0}^{N-1} \rho_n = \sum_{n=0}^{N-1} \frac{(-1)^n - Z_n}{2} = \frac{1}{2} \sum_{n=0}^{N-1} (-1)^n - \frac{1}{2} \sum_{n=0}^{N-1} Z_n.$$

The first term $\frac{1}{2} \sum_n (-1)^n$ depends only on the system size N and not on the quantum state. In particular, for even N the alternating sum cancels pairwise and vanishes, so $Q = -\frac{1}{2} \sum_n Z_n$. For odd N it contributes a fixed constant shift. In either case, conserving Q is therefore equivalent, up to an additive constant, to conserving the total Z magnetisation $\sum_n Z_n$.

This symmetry can be checked directly at the operator level by verifying that the Hamiltonian commutes with $\sum_k Z_k$. The only off-diagonal part of the spin Hamiltonian is the XY hopping,

$$-\frac{w}{2} \sum_n (X_n X_{n+1} + Y_n Y_{n+1}),$$

which can be written as $2(\sigma_n^+ \sigma_{n+1}^- + \sigma_n^- \sigma_{n+1}^+)$ and therefore only swaps neighbouring single-spin excitations, coupling $|01\rangle$ and $|10\rangle$ while leaving $|00\rangle$ and $|11\rangle$ unchanged. It follows that this term preserves the total number of occupied sites and hence commutes with $\sum_k Z_k$. The remaining terms H_m , H_E are diagonal in the Z basis and are functions only of commuting Z operators, so they also commute with $\sum_k Z_k$. Therefore

$$[H, \sum_k Z_k] = 0 \quad \Rightarrow \quad [H, Q] = 0,$$

confirming global charge conservation. Practically, this means the Hamiltonian block-diagonalises into sectors labelled by fixed Q or equivalently fixed

$\sum_n Z_n$, and variational ansätze or exact diagonalisation routines can exploit this number-preserving structure.

2.4 The staggered vacuum and the boundary flux sector

For $m > 0$ the mass term favours $n_n = 0$ on even sites and $n_n = 1$ on odd sites, giving the staggered vacuum

$$|\Omega\rangle = |0, 1, 0, 1, \dots\rangle.$$

On this state the charge density vanishes site by site: $\rho_n = n_n = 0$ on even sites and $\rho_n = n_n - 1 = 0$ on odd sites. Gauss's law then gives $E_n = E_L^{\text{bg}}$ on every physical link, so in the vacuum-flux sector $E_L^{\text{bg}} = 0$ the electric energy is exactly zero. This confirms that the staggered background subtraction in ρ_n serves its intended purpose: it makes the lattice vacuum locally neutral and free of spurious electric flux.

The boundary fluxes also provide a convenient way to prepare stringlike initial conditions. In the neutral sector $\sum_n \rho_n = 0$ the global constraint implies $E_R^{\text{bg}} = E_L^{\text{bg}}$, so choosing

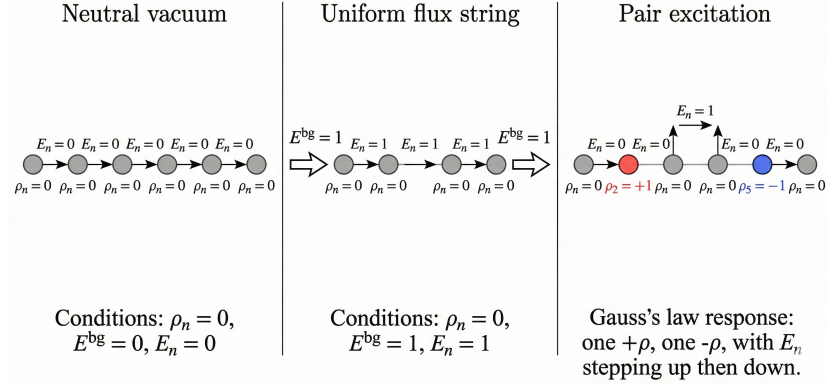
$$E_L^{\text{bg}} = E_R^{\text{bg}} = E^{\text{bg}}$$

threads the chain with a uniform background electric flux in the staggered vacuum. In that case $E_n = E^{\text{bg}}$ on every link and the electric-field energy stored in the string is

$$H_E = \frac{g^2}{2} \sum_{n=0}^{N-2} (E^{\text{bg}})^2 = \frac{g^2}{2} (N-1) (E^{\text{bg}})^2,$$

which grows linearly with system size, encoding confinement physics. In later real-time simulations, one can quench between flux sectors or between Hamiltonians to initiate string breaking dynamics.

“Three sectors side-by-side” mini-gallery



2.5 Verification: the $N = 4$ explicit matrix check

The integrated Hamiltonian contains off-diagonal terms from the XY hopping and long-range diagonal terms from the squared partial sums in H_E , with staggered signs and boundary-flux contributions. Convention errors such as misplaced signs, missing factors of $1/2$, or incorrect partial-sum indexing are easy to introduce and hard to spot by inspection.

For $N = 4$ the Hilbert space has dimension $2^4 = 16$, small enough to construct the full Hamiltonian matrix explicitly in the occupation-number basis $|n_0, n_1, n_2, n_3\rangle$. The check proceeds as follows:

1. Build the 16×16 matrix explicitly from the boxed Hamiltonian above, with sites $n = 0, 1, 2, 3$ and links $n = 0, 1, 2$.
2. Diagonalise and record the full spectrum.
3. Compare eigenvalues against those produced by the general ED builder used for larger N , with agreement to machine precision.
4. Compare eigenvectors in a fixed basis for at least the ground state and first excited state to validate phase conventions in the hopping terms.
5. Check block structure: the Hamiltonian must decompose into blocks labelled by the conserved quantum number $\sum_n Z_n$ equivalently by total charge Q .

Agreement across these checks validates the entire chain of manipulations from the original Kogut–Susskind Hamiltonian through gauge elimination, Jordan–Wigner mapping, and the cumulative-sum construction of the long-range interactions.

3. Open Quantum Systems for Quarkonium: From pNRQCD to a Lindblad Master Equation

The quantum simulation of lattice gauge theories (Gauge-Simulation Workstream (Schwinger / lattice dynamics) of this project) provides access to coherent, non-equilibrium dynamics that are fundamentally inaccessible to Euclidean Monte Carlo. A central real-time application in heavy-ion phenomenology is understanding how heavy quarkonium dissociates in the quark–gluon plasma (QGP). This has been addressed by a powerful effective framework: the open quantum system (OQS) approach derived from potential non-relativistic QCD (pNRQCD). This section develops the theoretical basis for Open-Quantum-Systems Workstream (pNRQCD-inspired Lindblad), following the derivation and first numerical applications in Brambilla, Escobedo, Soto and Vairo [1], and later extensions/implementations in Refs. [2, 3].

The goal is twofold: (i) to present the pNRQCD-to-Lindblad derivation in enough detail that the simplified models we implement (two-level and $1 \oplus 8$ nine-level systems) can be understood as controlled truncations of a rigorous

EFT framework; and (ii) to be transparent about which additional approximations our models introduce beyond Ref. [1].

References

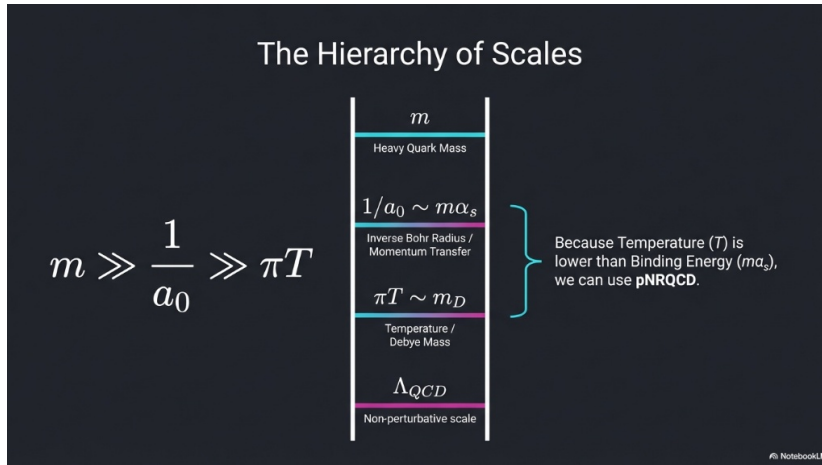
- [1] Brambilla, Escobedo, Soto, Vairo, *Phys. Rev. D* **96**, 034021 (2017); arXiv:1612.07248.
 - [2] Brambilla, Magorsch, Strickland, Vairo, Vander Griend, *Phys. Rev. D* **109**, 114016 (2024); arXiv:2403.15545.
 - [3] Brambilla, Magorsch, Vairo, arXiv:2508.11743 (2025).
-

3.1 The EFT hierarchy and scale separation

A heavy quark–antiquark pair ($Q\bar{Q}$) in the QGP involves a hierarchy of energy scales. The heavy-quark mass m (roughly 4.7 GeV for bottom) is the largest scale and is integrated out first, yielding NRQCD. The next scale is the inverse Bohr radius $1/a_0 \sim m\alpha_s$, which sets the typical relative momentum of a Coulombic bound state. In the scale hierarchy assumed in Ref. [1] (Eq. (1)),

$$m \gg \frac{1}{a_0} \sim m\alpha_s \gg \pi T \sim m_D \gg (\text{any other scale}),$$

pNRQCD is the EFT appropriate for a heavy $Q\bar{Q}$ pair at energies **below** the soft scale $m\alpha_s$ (the inverse Bohr radius) but still **above** the thermal scales. The theory is matched at the scale $m\alpha_s$ essentially as in vacuum by setting $T \rightarrow 0$, so the short-distance potentials are vacuum-like. Medium physics then enters only through lower-energy effects: thermal scales can require nonperturbative resummation in a strongly coupled plasma, and binding-energy effects may also be nonperturbative if the binding energy is $\lesssim \Lambda_{QCD}$.



pNRQCD degrees of freedom and Hamiltonians In pNRQCD the $Q\bar{Q}$ pair is described by explicit colour-singlet and colour-octet fields, S and O , evolving in the relative coordinate \mathbf{r} under singlet/octet Hamiltonians

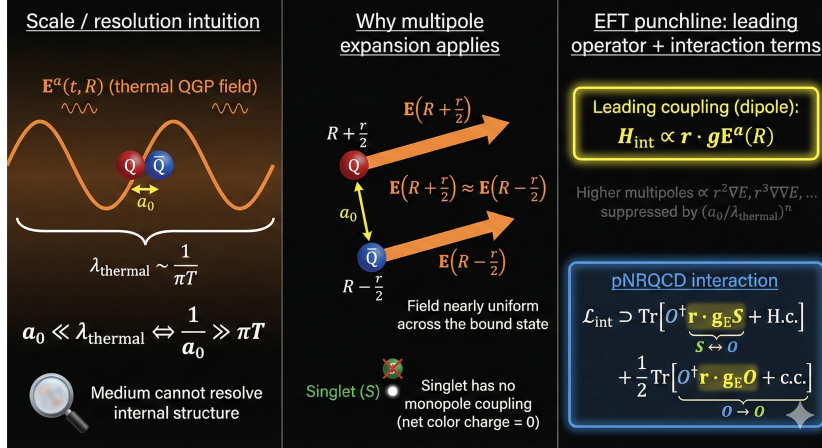
$$h_s = \frac{\mathbf{p}^2}{m} + V_s(r), \quad h_o = \frac{\mathbf{p}^2}{m} + V_o(r), \quad \mathbf{p} = -i\nabla_{\mathbf{r}}.$$

The regime considered in Ref. [1] focuses on compact Coulombic S-wave bottomonia. The corresponding short-distance Coulomb potentials are (Ref. [1], introductory discussion)

$$V_s(r) = -C_F \frac{\alpha_s}{r}, \quad V_o(r) = +\frac{\alpha_s}{2N_c r}, \quad C_F = \frac{N_c^2 - 1}{2N_c},$$

with $N_c = 3$ for QCD so $N_c^2 - 1 = 8$.

Multipole expansion and the pNRQCD Lagrangian The condition $\frac{1}{a_0} \gg \pi T$ is equivalent to $a_0 \ll \lambda_{\text{thermal}}$ with $\lambda_{\text{thermal}} \sim 1/(\pi T)$: the bound state is compact compared to the thermal wavelength. As a result, the QGP couples to the pair primarily through **long-wavelength chromoelectric fields**, and the interaction can be organized as a **multipole expansion** in \mathbf{r} .



At next-to-leading order in the multipole expansion (i.e. keeping terms up to $\mathcal{O}(r)$), the pNRQCD Lagrangian may be written as (paper Eq. (2))

$$\mathcal{L}_{\text{pNRQCD}} = \int d^3r \text{Tr}[S^\dagger(i\partial_0 - h_s)S + O^\dagger(iD_0 - h_o)O] + \int d^3r \text{Tr}[O^\dagger \underbrace{\mathbf{r} \cdot \mathbf{g}_E S}_{S \leftrightarrow O} + \text{H.c.}] + \frac{1}{2} \text{Tr}[O^\dagger \underbrace{\mathbf{r} \cdot \mathbf{g}_E O}_{O \rightarrow O} + \text{c.c.}] + \mathcal{L}_{\text{light}}.$$

Here \mathbf{r} is an **internal system variable** (the $Q\bar{Q}$ separation), while $g\mathbf{E}$ is a **medium (environment) operator** and g is the strong coupling. The singlet and octet fields are normalized as

$$S = S \frac{\mathbf{1}_c}{\sqrt{N_c}}, \quad O = \sqrt{2} O^a T^a,$$

and $\mathcal{L}_{\text{light}}$ denotes the QCD Lagrangian with light quarks only.

The covariant derivative acting on the octet field, D_0 , reflects that the octet transforms in the adjoint representation under gauge transformations at the center-of-mass coordinate \mathbf{R} . As noted in the quoted passage, it can be eliminated by a field redefinition using a Wilson line in time:

$$O \rightarrow \Omega O \Omega^\dagger, \quad \mathbf{E} \rightarrow \Omega \mathbf{E} \Omega^\dagger, \quad \Omega = \mathcal{P} \exp \left[-ig \int_{-\infty}^t ds A_0(s, \mathbf{R}) \right],$$

which is convenient in open-system derivations.

Finally, the two $\mathcal{O}(r)$ interaction structures encode the key physical processes:

$$\text{Tr} [O^\dagger \mathbf{r} \cdot g \mathbf{E} S + \text{H.c.}] + \frac{1}{2} \text{Tr} [O^\dagger \mathbf{r} \cdot g \mathbf{E} O + \text{c.c.}] .$$

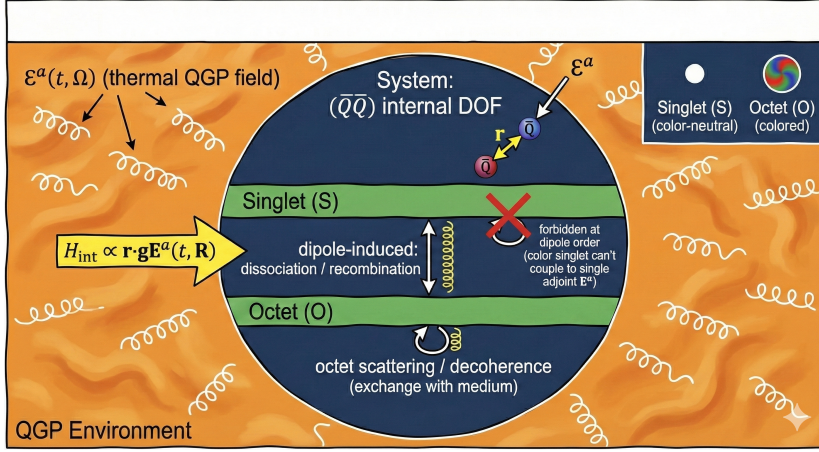
The dipole term $\mathbf{r} \cdot g \mathbf{E}$ which **couples system and environment**, and after tracing out the QGP it produces dissipative/decohering evolution of the reduced density matrix.

- **First term** ($O^\dagger \mathbf{r} \cdot g \mathbf{E} S + \text{H.c.}$): drives **singlet \leftrightarrow octet** transitions. Microscopically one may picture this as exchange of an adjoint gluonic excitation with the medium, but in the open-system description it is encoded in thermal field correlators rather than as an explicit on-shell “emitted gluon.” Physically this term underlies **dissociation** ($S \rightarrow O$) and **recombination** ($O \rightarrow S$).
- **Second term** ($O^\dagger \mathbf{r} \cdot g \mathbf{E} O + \text{c.c.}$): describes **octet \rightarrow octet** interactions with the QGP field. This does **not** mean the octet necessarily “produces a gluon” as a definite final-state particle; rather it represents **scattering with / exchange of energy and color with the medium**, leading (after tracing out the bath) to **color randomization, momentum diffusion, and decoherence** within the octet sector.

Notably, there is **no leading dipole term** of the form $S^\dagger \mathbf{r} \cdot g \mathbf{E} S$: a single chromoelectric field carries an adjoint color index and cannot connect a color-singlet to itself at this order. Singlet–singlet medium effects arise only indirectly (via $S \leftrightarrow O$) or from higher-order multipoles (e.g. two-field/polarizability terms).

Open-System Identification

- **System:** the $Q\bar{Q}$ relative coordinate and colour state (singlet or octet).
- **Environment:** the thermal QGP.
- **Coupling:** chromoelectric dipole interaction $\mathbf{r} \cdot g \mathbf{E}$.



3.2 Two non-perturbative parameters: κ and γ

In Ref. [1], the influence of the thermal medium enters through the chromoelectric dipole coupling in pNRQCD: the singlet interacts with the QGP by making virtual transitions $S \rightarrow O \rightarrow S$ induced by the medium chromoelectric field. At leading nontrivial order (second order in the dipole interaction), tracing over the thermal medium produces a **memory kernel** governed by a time-ordered chromoelectric correlator. In the singlet sector, this appears as a medium-induced self-energy (Ref. [1] Eq. (3))

$$\Sigma_s(t) = \frac{g^2}{6N_c} r^2 \int_{t_0}^t dt_2 \langle E_i^a(t, \mathbf{0}) E_i^a(t_2, \mathbf{0}) \rangle_T,$$

where isotropy has been used to contract spatial indices and the color normalization gives the prefactor $g^2/(6N_c)$. Physically, Σ_s encodes how QGP chromoelectric fluctuations dress the singlet: its **real part** generates dissipative broadening (loss of coherence/probability from the singlet sector) while its **imaginary part** generates a coherent dispersive energy shift (a Lamb-shift-like effect).

Following Ref. [1], we assume (i) $t - t_0$ is long compared to microscopic correlation times of the medium (Markov/long-time limit) and (ii) the medium cools quasistatically, $\dot{T}/T \sim 1/t$, so that the time integral may be approximated by an integral over all time separations. Writing the integral in terms of the time difference $s = t - t_2$ and extending to $(-\infty, \infty)$ defines two transport coefficients as the real and imaginary parts of the integrated time-ordered correlator:

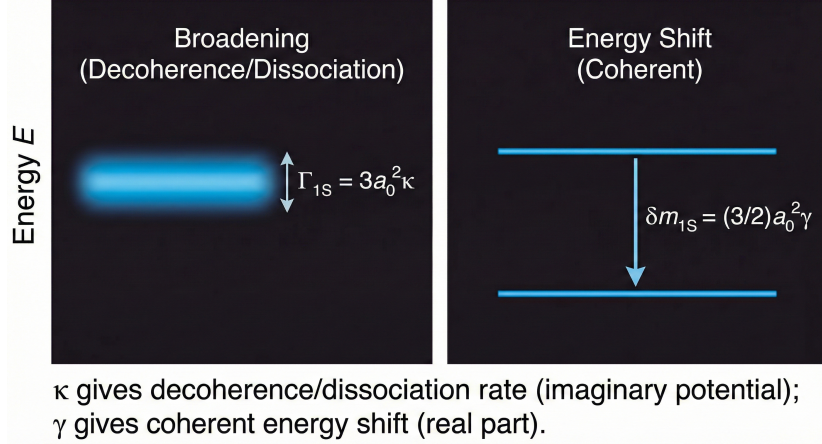
$$\kappa = \frac{g^2}{6N_c} \text{Re} \int_{-\infty}^{\infty} ds \langle \mathcal{T} E_i^a(s, \mathbf{0}) E_i^a(0, \mathbf{0}) \rangle_T, \quad \gamma = \frac{g^2}{6N_c} \text{Im} \int_{-\infty}^{\infty} ds \langle \mathcal{T} E_i^a(s, \mathbf{0}) E_i^a(0, \mathbf{0}) \rangle_T,$$

matching Ref. [1] Eqs. (5) and (8). Here κ is the heavy-quark momentum diffusion coefficient (the “noise strength” of chromoelectric fluctuations) and γ is its dispersive counterpart (the “reactive”/phase-shift part).

For a Coulombic $1S$ state, the medium effects at this order reduce to the expectation value of r^2 . Using the hydrogenic result $\langle r^2 \rangle_{1S} = 3a_0^2$, one finds that κ controls the in-medium width while γ controls the mass shift (Ref. [1] Eqs. (4), (7)):

$$\Gamma_{1S} = \kappa \langle r^2 \rangle_{1S} = 3a_0^2 \kappa, \quad \delta m_{1S} = \frac{\gamma}{2} \langle r^2 \rangle_{1S} = \frac{3}{2} a_0^2 \gamma.$$

Ref. [1] quotes the lattice-informed range $1.8 \lesssim \kappa/T^3 \lesssim 3.4$ (paper Eq. (6)), which implies $\Gamma \sim \mathcal{O}(100 \text{ MeV})$ at $T \sim 300 \text{ MeV}$ for $\Upsilon(1S)$ (paper discussion below Eq. (6)).



3.3 Coupled singlet–octet master equations and Lindblad form

In this section we derive the coupled singlet–octet master equations and their equivalent Lindblad (GKLS) form starting from the pNRQCD chromoelectric dipole coupling and applying the standard open-system reduction (Born–Markov, in the $\omega \rightarrow 0$ limit of Ref. [1]). We identify the kernel operators $\Sigma_{s,o}$ and the superoperators $\Xi_{so}, \Xi_{os}, \Xi_{oo}$, and then verify the Lindblad equivalence by explicit term-by-term algebra.

3.3.1 Setup: system, bath, and dipole couplings Take as **system** the QQ relative coordinate and its color state (singlet S or octet O). The **bath** is the thermal QGP (gluons and light quarks). At next-to-leading order in the multipole expansion, the pNRQCD interaction with the medium is linear in the chromoelectric field:

$$\mathcal{L}_{\text{int}} \supset \text{Tr}[O^\dagger \mathbf{r} \cdot g \mathbf{E} S + \text{H.c.}] + \frac{1}{2} \text{Tr}[O^\dagger \mathbf{r} \cdot g \mathbf{E} O + \text{c.c.}]$$

Equivalently, in Hamiltonian form the coupling may be written schematically as

$$H_{\text{int}}(t) = \sum_i A_i \otimes B_i(t),$$

with bath operators $B_i(t) \sim gE_i^a(t, \mathbf{R})$ and system operators $A_i \propto r^i$ multiplying color structures that (i) mediate $S \leftrightarrow O$ transitions and (ii) act within the octet sector. We use $r^2 \equiv r^i r^i$ with $i = 1, 2, 3$.

3.3.2 Born–Markov master equation (second order in H_{int}) Start from the von Neumann equation for the total density matrix ρ_{tot} :

$$\frac{d\rho_{\text{tot}}}{dt} = -i[H_S + H_B + H_{\text{int}}, \rho_{\text{tot}}].$$

Move to the interaction picture and expand in powers of H_{int} . The **first-order** contribution to the reduced dynamics is

$$\left. \frac{d\rho}{dt} \right|_{(1)} = -i \text{Tr}_B [H_{\text{int}}(t), \rho(t) \otimes \rho_B],$$

which is proportional to the bath one-point function $\langle B_i(t) \rangle_B$ in the decomposition $H_{\text{int}}(t) = \sum_i A_i \otimes B_i(t)$. For the pNRQCD dipole coupling, $B_i(t) \sim gE_i^a(t, \mathbf{R})$, and in a homogeneous, color-neutral thermal QGP one has $\langle E_i^a \rangle_T = 0$. Hence the first-order term vanishes (up to a trivial mean-field shift if a nonzero one-point function were present).

The **leading nonzero** medium effect therefore appears at **second order**, where the bath enters through its two-point correlator $\langle B_i(t)B_j(t-s) \rangle_T$. To see this explicitly, write the interaction in the factorized form

$$H_{\text{int}}(t) = \sum_{i,a} A_i^a(t) \otimes B_i^a(t), \quad B_i^a(t) \equiv gE_i^a(t, \mathbf{0}),$$

where $A_i^a(t)$ are system operators (built from r^i and color structures that mediate $S \leftrightarrow O$ or act within O) and $B_i^a(t)$ are bath operators. Inserting this into the Born–Markov second-order expression, the nested commutator expansion generates terms containing products of two bath operators, and tracing over the bath yields thermal two-point functions such as

$$\text{Tr}_B(\rho_B B_i^a(t) B_j^b(t-s)) = \langle B_i^a(t) B_j^b(t-s) \rangle_T \propto \langle E_i^a(t, \mathbf{0}) E_j^b(t-s, \mathbf{0}) \rangle_T.$$

Assuming weak system–bath coupling (Born approximation $\rho_{\text{tot}}(t) \approx \rho(t) \otimes \rho_B$ with thermal ρ_B) and a separation between the bath correlation time and the system evolution time (Markov approximation), the second-order expansion yields the standard time-local generator

$$\frac{d\rho}{dt} = - \int_0^\infty ds \text{Tr}_B[H_{\text{int}}(t), [H_{\text{int}}(t-s), \rho(t) \otimes \rho_B]].$$

Here $s \geq 0$ is the **time delay** (memory time): $t - s$ is an earlier time, and the integral over s weights how strongly the bath remains correlated between the two interaction events at times t and $t - s$. In practice, the bath correlator decays on a short microscopic timescale, so only small s contribute significantly in the Markov limit.

Because the bath state $\rho_B \propto e^{-H_B/T}$ is stationary, the correlator depends only on the time separation, so one may set

$$\langle E_i^a(t, \mathbf{0}) E_j^b(t-s, \mathbf{0}) \rangle_T = \langle E_i^a(s, \mathbf{0}) E_j^b(0, \mathbf{0}) \rangle_T.$$

Finally, isotropy and color symmetry of the thermal ensemble fix the tensor structure of the chromoelectric correlator at zero spatial separation. Define the (time-ordered) correlator

$$C_{ij}^{ab}(s) \equiv \langle \mathcal{T} E_i^a(s, \mathbf{0}) E_j^b(0, \mathbf{0}) \rangle_T.$$

Rotational invariance implies the spatial indices can only appear as δ_{ij} , and global color symmetry implies the adjoint indices can only appear as δ^{ab} . Therefore

$$C_{ij}^{ab}(s) = \delta_{ij} \delta^{ab} G(s),$$

for some scalar function $G(s)$ (up to a convention-dependent normalization). Here $G(s)$ is the thermal two-point correlator of the QGP chromoelectric field as a function of the time separation s ; it measures how strongly the medium's chromoelectric field at time s is correlated with the field at time 0.

More generally, the master equation involves the **frequency-resolved** response of the bath. In the interaction picture, the system operators evolve as

$$A_j^b(t-s) = e^{iH_S s} A_j^b(t) e^{-iH_S s},$$

so the integrand contains oscillatory factors $e^{\pm i\omega s}$, where ω is a **Bohr frequency** of the system (schematically $\omega \sim \Delta E$, e.g. singlet–octet energy splittings). Correspondingly, one may introduce the Fourier-transformed correlator

$$G(\omega) \sim \int_{-\infty}^{\infty} ds e^{i\omega s} \langle \mathcal{T} E_i^a(s, \mathbf{0}) E_i^a(0, \mathbf{0}) \rangle_T.$$

In the $\omega \rightarrow 0$ limit adopted in Ref. [1], the relevant energy splittings are treated as small on the timescale set by the bath correlation time, so the oscillatory

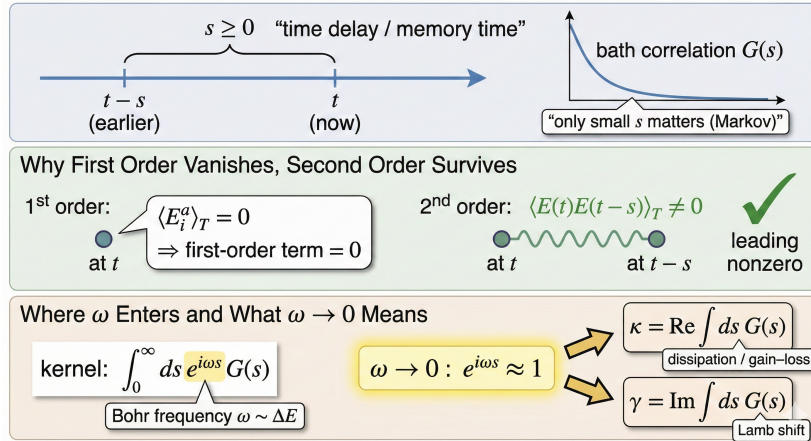
factors may be approximated by unity,

$$A_j^b(t-s) \approx A_j^b(t), \quad e^{\pm i\omega s} \approx 1.$$

The bath response then reduces to the two real, frequency-independent transport coefficients κ and γ defined as the real and imaginary parts of the time-integrated correlator:

$$\kappa = \frac{g^2}{6N_c} \text{Re} \int_{-\infty}^{\infty} ds G(s), \quad \gamma = \frac{g^2}{6N_c} \text{Im} \int_{-\infty}^{\infty} ds G(s).$$

The real part (κ) controls dissipative gain-loss terms, while the imaginary part (γ) produces the coherent “Lamb-shift” correction.



3.3.3 Block-diagonal structure and reduced variables

We work in the color basis $|s\rangle, |o\rangle$. In this basis the reduced density matrix has the general block form

$$\rho = \begin{pmatrix} \rho_{ss} & \rho_{so} \\ \rho_{os} & \rho_{oo} \end{pmatrix},$$

where $\rho_{ss} \equiv \rho_s$ and $\rho_{oo} \equiv \rho_o$ are the singlet- and octet-sector density matrices (operators on the relative-coordinate Hilbert space), while ρ_{so} and ρ_{os} encode **coherences** between singlet and octet sectors.

In the phenomenological situations of interest, the initial state is typically either a pure singlet bound state (so only ρ_s is nonzero) or a classical mixture of singlet and octet populations; in either case one has $\rho_{so} = \rho_{os} = 0$ initially. We therefore restrict to an initially block-diagonal reduced density matrix and write

$$\rho = \begin{pmatrix} \rho_s & 0 \\ 0 & \rho_o \end{pmatrix}.$$

This restriction is also **dynamically consistent** for the evolution derived below: after tracing over a color-neutral thermal bath and working in the Markovian limit, the resulting reduced dynamics does not generate singlet–octet coherences when they are absent initially, i.e. $\rho_{so}(t_0) = \rho_{os}(t_0) = 0$ implies $\rho_{so}(t) = \rho_{os}(t) = 0$ for all t . We will demonstrate this explicitly once the generator is written in its Lindblad (GKLS) form in §3.3.5 and verified by term-by-term algebra in §3.3.6.

Here ρ_s and ρ_o act on the relative-coordinate Hilbert space (with ρ_o representing the octet sector).

3.3.4 Coupled kernel equations: $\Sigma_{s,o}$ and Ξ After performing the bath trace and rewriting the resulting time-local generator in terms of the two transport coefficients κ and γ (defined in §3.2), one may cast the reduced evolution into GKLS form and then **project onto the singlet and octet blocks** of $\rho = \text{diag}(\rho_s, \rho_o)$. This block projection yields the coupled kernel equations of Ref. [1] (Eqs. (10)–(11)):

$$\begin{aligned}\frac{d\rho_s}{dt} &= -i[h_s, \rho_s] - \Sigma_s \rho_s - \rho_s \Sigma_s^\dagger + \Xi_{so}(\rho_o), \\ \frac{d\rho_o}{dt} &= -i[h_o, \rho_o] - \Sigma_o \rho_o - \rho_o \Sigma_o^\dagger + \Xi_{os}(\rho_s) + \Xi_{oo}(\rho_o).\end{aligned}$$

Self-energies. The operators Σ_s and Σ_o collect the in-sector “loss” terms (from the anticommutator pieces of the GKLS dissipator) together with the dispersive contribution (from the imaginary part of the same bath integral):

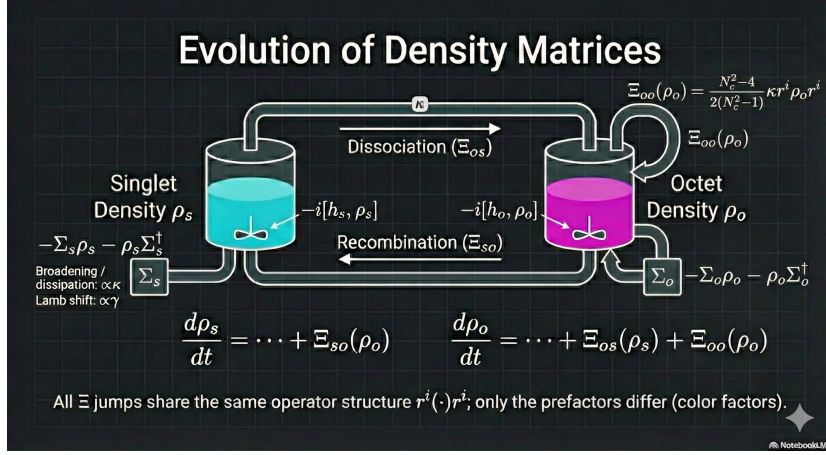
$$\Sigma_s = \frac{r^2}{2}(\kappa + i\gamma), \quad \Sigma_o = \frac{N_c^2 - 2}{2(N_c^2 - 1)} \frac{r^2}{2}(\kappa + i\gamma).$$

The different coefficient in Σ_o is a color factor: in the octet sector the total coefficient receives contributions from both $S \leftrightarrow O$ dipole transitions and $O \rightarrow O$ dipole scattering, which combine to $(N_c^2 - 2)/(2(N_c^2 - 1))$.

Gain kernels. The superoperators Ξ arise from the $C\rho C^\dagger$ (“gain”) part of the GKLS dissipator and encode probability flow between color sectors:

$$\Xi_{os}(\rho_s) = \kappa r^i \rho_s r^i, \quad \Xi_{so}(\rho_o) = \frac{1}{N_c^2 - 1} \kappa r^i \rho_o r^i, \quad \Xi_{oo}(\rho_o) = \frac{N_c^2 - 4}{2(N_c^2 - 1)} \kappa r^i \rho_o r^i.$$

All three share the same operator sandwich $r^i(\cdot)r^i$; only the color prefactors differ.



3.3.5 Lindblad (GKLS) form Casting the singlet–octet evolution in Lindblad (GKLS) form makes the open-system nature of quarkonium propagation explicit: it guarantees a completely positive, trace-preserving time evolution so the reduced density matrix remains physical throughout. At the same time, it cleanly separates coherent medium effects (via an effective Hamiltonian/Lamb shift) from irreversible dynamics (via the dissipator), and rewrites the (Ξ) kernels as transparent “jump” processes with well-defined collapse operators. This structure also makes general properties—such as the preservation of singlet/octet block diagonality—straightforward to see and to use in practical implementations.

The coupled kernel equations are equivalent to the standard GKLS/Lindblad master equation (Ref. [1] Eq. (17))

$$\frac{d\rho}{dt} = -i[H_{\text{eff}}, \rho] + \sum_n \left(C_n \rho C_n^\dagger - \frac{1}{2} \{C_n^\dagger C_n, \rho\} \right).$$

This form arises by starting from the von Neumann equation for the full system+bath density matrix,

$$\frac{d\rho_{\text{tot}}}{dt} = -i[H_S + H_B + H_{\text{int}}, \rho_{\text{tot}}],$$

and tracing out the bath in the Born–Markov approximation. The reduced generator always contains a coherent piece that looks like unitary evolution, $-i[H_S, \rho]$, plus a bath-induced **Lamb-shift** correction coming from the **imaginary (principal-value) part** of the bath correlation integral. Absorbing this renormalization into an effective Hamiltonian $H_{\text{eff}} = H_S + H_{\text{LS}}$ gives the coherent term $-i[H_{\text{eff}}, \rho]$. In the present pNRQCD setting, the Lamb shift is

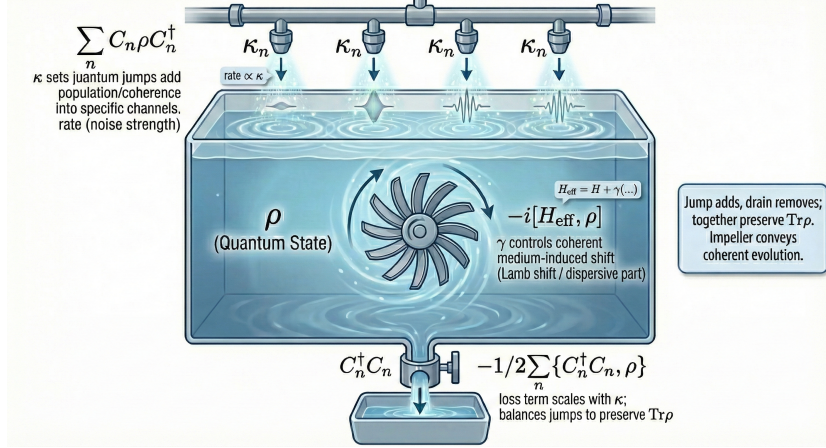
controlled by γ and yields the effective Hamiltonian (Ref. [1] Eq. (19))

$$H_{\text{eff}} = \begin{pmatrix} h_s & 0 \\ 0 & h_o \end{pmatrix} + \frac{r^2}{2}\gamma \begin{pmatrix} 1 & 0 \\ 0 & \frac{N_c^2-2}{2(N_c^2-1)} \end{pmatrix}.$$

The same second-order Born–Markov reduction also produces dissipative terms governed by the **real part** of the bath two-point function, which encode irreversible decoherence/dissipation. Requiring the reduced dynamics to be trace preserving and completely positive implies that these terms can be written in GKLS form using “collapse” (jump) operators C_n . In pNRQCD they are proportional to $r^i \sqrt{\kappa}$ (times color matrices), so κ sets the overall strength of dissipation. A convenient choice (Ref. [1] Eqs. (20)–(21)) uses two color structures times the three spatial components $i = 1, 2, 3$, giving six operators:

$$C_i^{(0)} = \sqrt{\kappa} r^i \begin{pmatrix} 0 & \frac{1}{\sqrt{N_c^2-1}} \\ 1 & 0 \end{pmatrix}, \quad C_i^{(1)} = \sqrt{\kappa} r^i \begin{pmatrix} 0 & 0 \\ 0 & \sqrt{\frac{N_c^2-4}{2(N_c^2-1)}} \end{pmatrix}, \quad i = 1, 2, 3.$$

With this choice, the $C\rho C^\dagger$ (“gain”) terms reproduce the superoperators Ξ_{so} , Ξ_{os} , and Ξ_{oo} , while the anticommutator terms $-\frac{1}{2}\{C^\dagger C, \rho\}$ reproduce the κ -parts of Σ_s and Σ_o . The dispersive coefficient γ may equivalently be packaged as the imaginary part of $\Sigma_{s,o}$ or as the explicit Hamiltonian correction in H_{eff} above; both representations are identical after regrouping terms.



Moreover, H_{eff} is block diagonal in the $|s\rangle, |o\rangle$ basis, so the coherent contribution $-i[H_{\text{eff}}, \rho]$ cannot generate off-diagonal blocks if they vanish initially. And with the chosen collapse operators, the dissipator

$$\sum_n \left(C_n \rho C_n^\dagger - \frac{1}{2} \{C_n^\dagger C_n, \rho\} \right)$$

maps diagonal blocks back into diagonal blocks: it produces gain terms of the form $r^i \rho_s r^i$ into the octet sector and $r^i \rho_o r^i$ into the singlet sector, while averag-

ing over the color-neutral bath removes any persistent S - O coherences. Equivalently, if $\rho_{so}(t_0) = \rho_{os}(t_0) = 0$, then the equations of motion give $\dot{\rho}_{so} = \dot{\rho}_{os} = 0$, and the reduced density matrix remains block diagonal for all times.

3.3.6 Explicit verification: term-by-term algebra (kernel notation)

We verify that the Lindblad dissipator

$$\mathcal{D}[\rho] = \sum_n \left(C_n \rho C_n^\dagger - \frac{1}{2} \{ C_n^\dagger C_n, \rho \} \right)$$

reproduces the kernels $\Xi_{so}, \Xi_{os}, \Xi_{oo}$ and the κ -parts of Σ_s, Σ_o .

Define

$$a \equiv \frac{1}{\sqrt{N_c^2 - 1}}, \quad b \equiv \sqrt{\frac{N_c^2 - 4}{2(N_c^2 - 1)}}, \quad M \equiv \begin{pmatrix} 0 & a \\ 1 & 0 \end{pmatrix}, \quad D \equiv \begin{pmatrix} 0 & 0 \\ 0 & b \end{pmatrix},$$

so that $C_i^{(0)} = \sqrt{\kappa} r^i M$ and $C_i^{(1)} = \sqrt{\kappa} r^i D$.

(A) Gain terms $\Rightarrow \Xi$. Using $\rho = \text{diag}(\rho_s, \rho_o)$,

$$M\rho M^\dagger = \begin{pmatrix} a^2 \rho_o & 0 \\ 0 & \rho_s \end{pmatrix}, \quad D\rho D^\dagger = \begin{pmatrix} 0 & 0 \\ 0 & b^2 \rho_o \end{pmatrix}.$$

Hence

$$C_i^{(0)} \rho C_i^{(0)\dagger} = \kappa r^i (M\rho M^\dagger) r^i = \kappa \begin{pmatrix} a^2 r^i \rho_o r^i & 0 \\ 0 & r^i \rho_s r^i \end{pmatrix}, \quad C_i^{(1)} \rho C_i^{(1)\dagger} = \kappa r^i (D\rho D^\dagger) r^i = \kappa \begin{pmatrix} 0 & 0 \\ 0 & b^2 r^i \rho_o r^i \end{pmatrix}.$$

Summing over i and inserting $a^2 = 1/(N_c^2 - 1)$ and $b^2 = (N_c^2 - 4)/(2(N_c^2 - 1))$ gives exactly

$$\Xi_{so}(\rho_o) = \frac{\kappa}{N_c^2 - 1} r^i \rho_o r^i, \quad \Xi_{os}(\rho_s) = \kappa r^i \rho_s r^i, \quad \Xi_{oo}(\rho_o) = \frac{N_c^2 - 4}{2(N_c^2 - 1)} \kappa r^i \rho_o r^i.$$

(B) Loss terms $\Rightarrow \Sigma^{(\kappa)}$. First compute

$$\sum_i C_i^{(0)\dagger} C_i^{(0)} = \kappa r^2 \begin{pmatrix} 1 & 0 \\ 0 & a^2 \end{pmatrix}, \quad \sum_i C_i^{(1)\dagger} C_i^{(1)} = \kappa r^2 \begin{pmatrix} 0 & 0 \\ 0 & b^2 \end{pmatrix}.$$

Adding them and using $a^2 + b^2 = (N_c^2 - 2)/(2(N_c^2 - 1))$ yields

$$\sum_{i,\alpha} C_i^{(\alpha)\dagger} C_i^{(\alpha)} = \kappa r^2 \begin{pmatrix} 1 & 0 \\ 0 & \frac{N_c^2 - 2}{2(N_c^2 - 1)} \end{pmatrix}.$$

Therefore

$$-\frac{1}{2}\{\sum_{i,\alpha} C_i^{(\alpha)\dagger} C_i^{(\alpha)}, \rho\} = \Sigma^{(\kappa)}\rho - \rho\Sigma^{(\kappa)},$$

with

$$\Sigma_s^{(\kappa)} = \frac{r^2}{2}\kappa, \quad \Sigma_o^{(\kappa)} = \frac{N_c^2 - 2}{2(N_c^2 - 1)} \frac{r^2}{2}\kappa.$$

Including the dispersive part amounts to $\kappa \rightarrow (\kappa + i\gamma)$, giving the full Σ_s and Σ_o quoted in §3.3.4, or equivalently the Hamiltonian shift in H_{eff} .

Interpretation (summary)

- $\Sigma_{s,o}$ encode in-sector dissipation (via κ) and dispersive shifts (via γ).
- Ξ_{os} describes singlet \rightarrow octet production (dissociation).
- Ξ_{so} describes octet \rightarrow singlet production (recombination), with the $1/(N_c^2 - 1)$ normalization reflecting octet multiplicity.
- Ξ_{oo} describes octet \rightarrow octet scattering/decoherence.

The Lindblad (GKLS) structure guarantees complete positivity of the reduced evolution.

3.4 From pNRQCD to simplified models: controlled truncations

The full pNRQCD master equation acts on an infinite-dimensional Hilbert space (relative-coordinate wavefunctions in each colour sector). Our numerical implementations are finite-dimensional truncations that preserve the essential colour structure and gain–loss physics while projecting out spatial dynamics.

Two-level model We project the singlet and octet density matrices onto fixed spatial modes:

$$\rho_s(t) \approx p_s(t)|\psi_s\rangle\langle\psi_s|, \quad \rho_o(t) \approx p_o(t)|\psi_o\rangle\langle\psi_o|,$$

where $|\psi_s\rangle$ is a chosen singlet bound-state mode (e.g. vacuum $1S$) and $|\psi_o\rangle$ is an **effective octet mode** representing the octet sector. We then replace spatial operators by expectation values $r^i \rho r^i \rightarrow \langle r^2 \rangle p$. This reduces the coupled equations to population rate equations:

$$\dot{p}_s = -\Gamma_{s \rightarrow o} p_s + \Gamma_{o \rightarrow s} p_o,$$

with effective rates inherited from the pNRQCD kernels:

$$\Gamma_{s \rightarrow o} = \kappa \langle r^2 \rangle_s, \quad \Gamma_{o \rightarrow s} = \frac{\kappa}{N_c^2 - 1} \langle r^2 \rangle_o.$$

The factor $1/(N_c^2 - 1) = 1/8$ reflects octet multiplicity and associated colour normalization in the singlet \leftrightarrow octet kernels (compare Ξ_{so} and the definition/normalization of the octet sector in Ref. [1]) .

Important distinction: Bose factors versus the $\omega \rightarrow 0$ reduction. Ref. [1] works in a limit where energy-dependent oscillatory factors can be neglected, collapsing the bath response into the frequency-independent coefficients $\kappa(t)$ and $\gamma(t)$. In that reduced description, transition rates are not written in explicitly $\omega = \Delta E$ -resolved (Bose-factor) form. In our toy model, we *assume* an energy-resolved bath response at $\omega = \Delta E$ and impose detailed balance using Bose-Einstein occupation numbers

$$n_{\text{th}}(\Delta E, T) = \frac{1}{e^{\Delta E/T} - 1},$$

with dissociation $\propto n_{\text{th}}$ and recombination $\propto 1 + n_{\text{th}}$. For $\Delta E \ll T$, upward/downward rates become nearly equal ($n_{\text{th}} \gg 1$); with appropriate matching of the overall rate scale (Γ_0 to an effective $\kappa\langle r^2 \rangle$), the Bose-factor model reproduces the near-equipartition behavior of the $\omega \rightarrow 0$ truncation.

Throughout the numerical implementation we use a phenomenological rate scale Γ_0 , calibrated so that the total in-medium width lies in the ballpark suggested by Ref. [1] (e.g. $\Gamma \sim \mathcal{O}(100 \text{ MeV})$ at $T \sim 300 \text{ MeV}$) .

Nine-level model (1 \oplus 8) Motivated by the explicit octet multiplicity $N_c^2 - 1 = 8$ and the colour factors in Ξ_{so} (Ref.[1] Eq. (14)) , we represent the octet degeneracy explicitly: one singlet $|s\rangle$ and eight octet states $|o_a\rangle$, $a = 1, \dots, 8$.

Per channel we take

$$L_a^{\text{diss}} = \sqrt{\Gamma_0 \cdot n_{\text{th}}} |o_a\rangle\langle s|, \quad L_a^{\text{rec}} = \sqrt{\Gamma_0(1 + n_{\text{th}})} |s\rangle\langle o_a|,$$

Then:

- **Per-channel dissociation rate:** $\Gamma_{\text{per}}^{\text{diss}} = \Gamma_0 n_{\text{th}}$
- **Total dissociation rate out of the singlet:** $\Gamma_{\text{tot}}^{\text{diss}} = 8\Gamma_0 n_{\text{th}}$
- **Recombination rate from any single octet state:** $\Gamma_{\text{per}}^{\text{rec}} = \Gamma_0(1 + n_{\text{th}})$

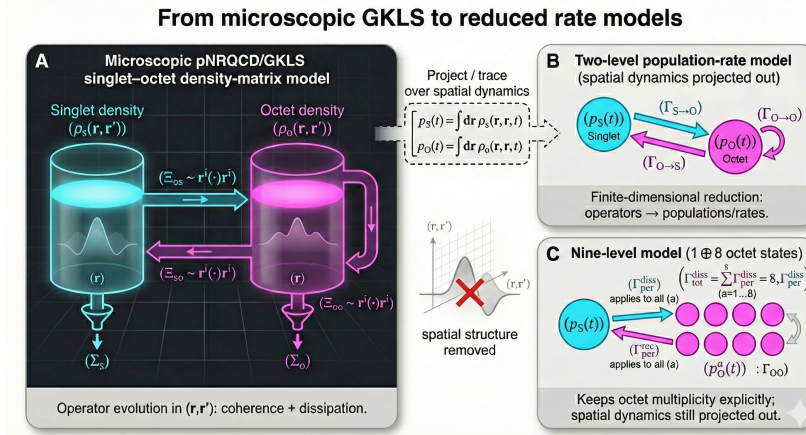
At equilibrium, detailed balance holds channel-by-channel:

$$p_s^{\text{eq}} \Gamma_0 n_{\text{th}} = p_{o_a}^{\text{eq}} \Gamma_0(1 + n_{\text{th}}) \Rightarrow \frac{p_s^{\text{eq}}}{p_{o_a}^{\text{eq}}} = \frac{1 + n_{\text{th}}}{n_{\text{th}}} = e^{\Delta E/T}.$$

Defining the total octet population $p_o^{\text{eq}} = 8p_{o_a}^{\text{eq}}$, this implies

$$\frac{p_s^{\text{eq}}}{p_o^{\text{eq}}} = \frac{e^{\Delta E/T}}{8}, \quad p_s^{\text{eq}} = \frac{1}{1 + 8e^{-\Delta E/T}}.$$

In the high-temperature limit $T \gg \Delta E$, $p_s^{\text{eq}} \rightarrow 1/9$.



3.5 Summary: what the simplified models capture and what they omit

Feature	Full pNRQCD / OQS (Ref. [1])	Our 9-level model
Colour structure (singlet + octet)	Yes	Yes (explicit $1 \oplus 8$)
Detailed balance / thermalization	Yes (implicit via thermal correlators; explicit ω -resolved form in more general treatments)	Yes (imposed via Bose factors)
Octet multiplicity $N_c^2 - 1 = 8$	Yes (in kernels/normalization)	Yes (8 explicit channels)
Spatial wavefunction dynamics $\rho_{s,o}(\mathbf{r}, \mathbf{r}')$	Yes	No (single-mode projection)
r -dependent dipole transitions $(C_n \propto r^i)$	Yes (six collapse ops in 3D)	No (absorbed into Γ_0)
Dispersive shift γ	Yes (in H_{eff})	No (set to the baseline choice $\gamma = 0$; absorbed into an effective ΔE at population level)
Medium evolution $\kappa(t), \gamma(t)$	Yes	No (fixed T)

The omissions are deliberate: we retain the minimal structure needed to reproduce qualitative phenomenology—temperature-dependent dissociation via $n_{\text{th}}(\Delta E, T)$, colour-factor-driven equilibration through the explicit $1 \oplus 8$ multiplicity and detailed-balance rates, and sequential suppression by comparing different ΔE —while keeping the model tractable for a focused demonstration.

In particular, setting γ aside does **not** undermine the value of the project, provided we are explicit about scope. Ref. [1] emphasizes that the full phenomenological output depends crucially on both κ and γ , and that while κ has at least been computed in (quenched) lattice QCD, γ has not and remains a major uncertainty. Consistent with this, Ref. [1] adopts the explicit baseline choice $\gamma = 0$ for its illustrative bottomonium results, noting that the choice is “arbitrary” in the absence of a non-perturbative determination.

3.6 Physical units

We quote energies in MeV and time in fm/c , using $\hbar c = 197.3 \text{ MeV}\cdot\text{fm}$, enabling direct comparison to QGP lifetimes of $\sim 5\text{--}10 \text{ fm}/c$ in Pb–Pb collisions. The phenomenological rate scale Γ_0 is chosen such that typical dissociation widths fall in the range $\sim 50\text{--}200 \text{ MeV}$ around $T \sim 400 \text{ MeV}$, consistent with the order-of-magnitude widths discussed in Ref. [1]. This corresponds to characteristic timescales $\tau \sim \hbar/\Gamma \sim 1\text{--}4 \text{ fm}/c$, comparable to the QGP lifetime and hence phenomenologically relevant.

Summary of Validation Baseline Deliverables

- **Pure gauge U(1):** exact Wilson-loop area law used to validate Monte Carlo simulations.
- **Schwinger model Hamiltonian:** gauge-eliminated spin-chain derivation and $N = 4$ explicit matrix verification.
- **OQS quarkonium model:** singlet-octet Lindblad dynamics (2-level and 9-level) with correct detailed balance, color degeneracy, and physical timescales.